WEP
Warwick
Evans
Publishing

International Journal of Electric Power and Energy Studies
ISSN: 3006-2004 (Print), ISSN: 3006-0826 (Online) | Volume 4, Number 1, Year 2025
DOI: https://doi.org/10.62051/ijepes.v4n1.06
Journal homepage: https://wepub.org/index.php/IJEPES/index

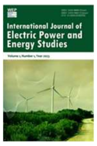

Research of Children Dyslexia Classification Recognition based on Graph Convolutional Neural Networks

Maoyun Wang

School of Computer Science and Technology, Taiyuan Normal University, Jinzhong, China

ABSTRACT

Developmental dyslexia is a common neurodevelopmental disorder that significantly affects children' normal learning and life. Early identification and intervention are crucial for patients. However, current models for classifying dyslexia fail to automatically extract features based on patient data and overlook the interrelationships between brain nodes in patients. Therefore, this paper proposes a graph convolutional neural network model that constructs a brain network from patients' fMRI data as an adjacency matrix, calculates node feature matrices, trains GCN models for classification, and achieves the diagnosis of dyslexia patients. Experimental results show that the model has an identification accuracy of 94%, precision of 95%, recall of 94%, and F1 score of 94%. This study provides a new approach for identifying and diagnosing dyslexia, which is beneficial for early intervention in dyslexia patients.

KEYWORDS

fMRI; Developmental Dyslexia; GCN; Feature Extraction.

1. INTRODUCTION

Developmental Dyslexia (DD)[1], also referred to as reading disorder, reading disability, or dyslexia, is a common learning difficulty that affects the development of an individual's reading and comprehension abilities. DD is a neurodevelopmental disorder that typically manifests during childhood[2]. It is not caused by intellectual deficits, inadequate education, or environmental factors but rather by differences in how the nervous system processes written language compared to neurotypical individuals. The exact etiology of DD remains unclear, though abnormalities in visual and auditory neural development are considered key contributing factors[3]. DD can have long-term negative impacts on individuals across multiple domains, including academic performance, social interaction, and emotional well-being[4].In China, the estimated prevalence of DD ranges from 4% to 10%[5], indicating that over 10 million children are affected. Therefore, it is essential to establish accurate and effective predictive models for Chinese children with DD, which would facilitate early diagnosis and intervention.

In recent years, significant progress has been made in diagnostic methods for developmental dyslexia (DD), including eye-tracking[6],electroencephalography (EEG)[7],standardized test scores[8], and functional magnetic resonance imaging (fMRI)[9]. These approaches have provided researchers with advanced tools and data to better understand the neural underpinnings and diagnostic markers of DD. Among these, fMRI—a non-invasive technique offering high spatial resolution—has been widely adopted in DD research, as it enables detailed mapping of regional brain activity.In early studies on dyslexia identification, combining feature extraction methods with machine learning algorithms was a primary approach to investigating DD's pathogenesis. For instance, Cui et al.[10] extracted white matter features from MRI data and trained a linear support vector machine (LSVM) classifier, achieving a classification accuracy of 83.61%. Similarly, Płoński et al.[11] employed multivariate machine learning on cortical morphological features derived from MRI data, including volumetric(volume, thickness, surface area) and geometric measurements (folding index, mean curvature), reporting an AUC of 0.66 and ACC of 0.65.

Compared to traditional machine learning, the primary advantage of deep learning lies in its ability to automatically learn hierarchical feature representations directly from raw data, thereby eliminating the need for manual feature engineering-a step inherent to conventional machine learning models[12]. Deep learning has progressively emerged as a pivotal technology for identifying neurodevelopmental disorders, including dyslexia.For instance,Usman et al.[13]developed a pixel bitstream encoder based on a residue number system (RNS) with a specialized modulus set to encrypt the 7-bit binary values of each pixel in MRI datasets, ensuring data privacy protection. They then employed a cascaded deep convolutional neural network (CNN) to classify developmental dyslexia, achieving an accuracy of 73.2%.Similarly,Silva et al.[14] utilized a CNN-based approach to classify individuals with DD using fMRI data, attaining a remarkable accuracy of 94.8%. Additionally, they incorporated visualization techniques to highlight the discriminative features involved in classification, enabling experts to gain deeper insights into the model's decision-making process.

However, in the field of medical deep learning, traditional convolutional neural networks cannot process non-Euclidean spatial data. The emergence of Graph Convolutional Neural Networks (GCNs)[15] effectively addresses this limitation. GCNs are a deep learning method that combines CNNs with graph theory, performing convolutional operations on graphs to integrate node feature information with inter-node relationships, thereby fully and deeply characterizing graph-structured data[16]. GCNs have been widely applied in disease detection, particularly for brain disorders[17]. Zhang et al.[18] proposed a Memory Graph Convolutional Network (MemGCN) that utilized features extracted from patients' clinical records and neuroimaging data to achieve Parkinson's disease detection. Liu et al.[19] used resting-state EEG data, dividing each subject's EEG data into different frequency bands and segment lengths, constructing brain networks using various functional connectivity metrics, and then training a GCN model with node feature matrices composed of temporal-frequency domain features of EEG signals and local brain network characteristics. Arya et al.[20] leveraged information from structural and functional MRI data to construct graph edges and nodes, extracted features from brain parcellations, and trained a GCN model, which enhanced the generalization capability and performance of autism classification. Yang et al.[21] proposed an SGCN model for brain disorder detection that employed two GCNs for pairwise matching learning, achieving better performance than single GCNs and shallow CNNs.

Therefore, this study proposes a graph convolutional neural network-based approach that constructs brain networks from patients' fMRI data as adjacency matrices, computes node feature matrices, and trains a GCN model for classification, thereby achieving the identification and diagnosis of individuals with developmental dyslexia.

2. METHOD

2.1. Data

2.1.1. Participants

The study recruited fourth and fifth-grade students from an elementary school in Beijing, China, screening for both developmental dyslexia and control groups. Participants' reading abilities were assessed using a character reading test, teacher evaluations, and performance in Chinese language courses. The test included Chinese characters selected from both curriculum materials and beyond-curriculum sources, requiring students to read aloud as many characters as possible within 90 seconds with maximum accuracy. Reading accuracy served as the primary metric for evaluating reading performance. Students scoring 1.5 standard deviations below the mean were classified as having dyslexia, while those scoring 1.5 standard deviations above the mean comprised the control group. For the functional magnetic resonance imaging (fMRI) study, 10 Participants with dyslexia and 10 control Participants were included. Demographic and statistical information is presented in Table 1.

Table 1. Demographic data table of Participants

Characteristic	Dyslexia Group (n=10)	Control Group (n=10)	**Statistical Value**
Mean Age	10 years 3 months	10 years 3 months	
Reading Performance	32.6 ± 13.73	119.5 ± 15364	t=14.33 p<0.001
Gender (M/F)	7/3	7/3	
Nonverbal IQ	74 ± 18.07	70.5 ± 15.35	t=-0.56 p=0.58

2.1.2. Stimuli and Procedure

Participants performed a homophone judgment task during the experiment:In the 0-back condition, a target Chinese character was specified on the instruction page of each run, and Participants were required to determine whether the currently presented character shared the same pronunciation as this pre-specified character. In the 2-back condition, Participants judged whether the current character shared the same pronunciation as the character presented two trials earlier.The task consisted of four runs. Each run began with 2-second instructions and included eight trials. During each trial, a Chinese character was displayed at the center of the screen for 500 ms, followed by a 2500 ms blank screen for response. All experimental runs were interleaved with 12-second fixation blocks, during which Participants focused their gaze on a central crosshair.Responses were recorded using an fMRI-compatible response box, with Participants indicating "yes" or "no" by pressing either the right or left button with their index finger.

2.2. Data Preprocessing

The study utilized the FMRIB Software Library for image preprocessing[22]. Functional images from each participant underwent slice-timing correction and spatial normalization. Specifically, the EPI template from ICBM152 stereotactic space served as the reference for normalization, with subsequent resampling to adjust each voxel to 3 mm × 3 mm × 3 mm isotropic dimensions. Spatial smoothing was applied using a 6 mm full-width-at-half-maximum isotropic Gaussian kernel to reduce noise and enhance signal-to-noise ratio. Following motion correction, the first three volumes of each run were discarded to account for transient hemodynamic effects prior to task onset.

2.3. Graph Convolutional Neural Network

The overall architecture of the model is illustrated in Fig. 1. Using participants' fMRI data, we computed Pearson correlation coefficient matrices to construct brain network adjacency matrices as input for the GCN model.

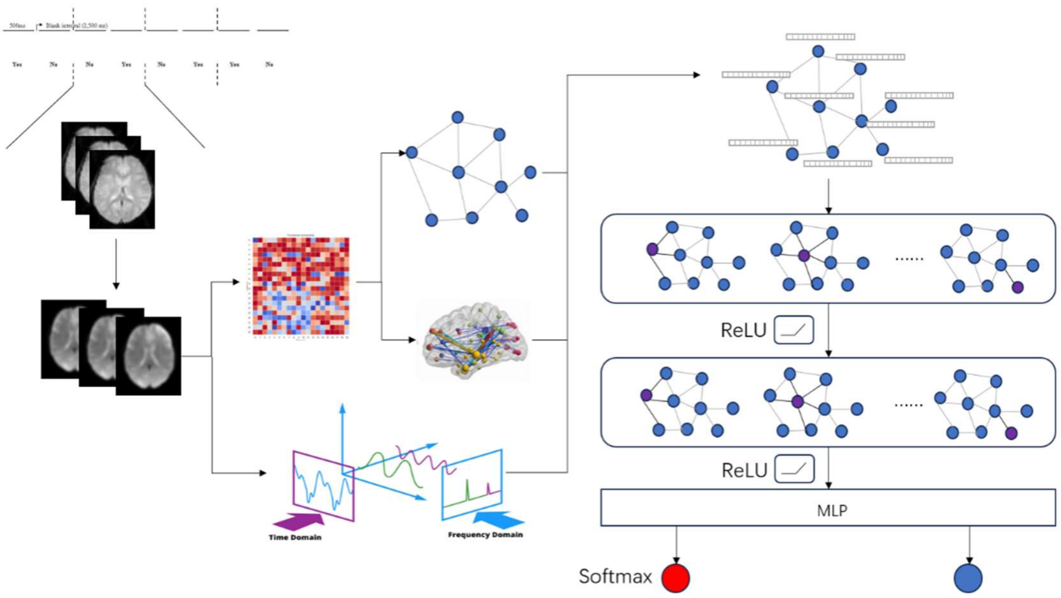

Fig. 1 Model Structure Diagram

Node features were represented by combining time-domain features, frequency-domain features, and local brain network characteristics. For time-domain features, we computed the mean, variance, minimum (MIN), maximum (MAX), standard deviation (STD), peak value, skewness, and kurtosis. For frequency-domain features, we calculated the average power spectral density of the fMRI data. For local brain network features, we constructed binary undirected networks and computed degree centrality, betweenness centrality, clustering coefficient, global efficiency, local efficiency, and shortest path length[23], resulting in 14 feature dimensions per node.

Our GCN model consisted of two GCN layers. The first GCN layer performed graph convolution operations using the brain network's adjacency matrix A and node feature matrix X, where each node aggregated features from neighboring nodes and then updated its own node features. In the second GCN layer, each node's features incorporated both its own characteristics and information from all first-order neighbors, continuing to aggregate new node features in the same manner. The graph convolution operation is defined by Equation (1).

$$Z = \widetilde{D}^{-\frac{1}{2}}\tilde{A}\widetilde{D}^{-\frac{1}{2}}X\Theta \tag{1}$$

Here,$\tilde{A} = A + I$, where I represents the identity matrix, and $\widetilde{D}$ denotes the degree matrix with $\widetilde{D}_{ii} = \sum_j \tilde{A}_{ij}$.

Through multiple graph convolutional layers, the model progressively aggregates local information to derive more comprehensive representations. For a multi-layer graph convolution, its layer-wise propagation rule is formally defined by Equation (2):

$$H^{(l+1)} = \sigma\left(\widetilde{D}^{-\frac{1}{2}}\tilde{A}\widetilde{D}^{-\frac{1}{2}}H^{(l)}W^{(l)}\right) \tag{2}$$

Here, l denotes the convolutional layer number, $H^{(l)}$ represents the input node feature matrix where $H^{(l)} \in R^{N\times d}$,with N being the number of nodes in the brain network and d indicating the feature dimension of each node. $W^{(l)}$ is the weight matrix, $W^{(l)} \in R^{d\times F}$.while $H^{(l+1)}$ corresponds to the output feature matrix, $H^{(l+1)} \in R^{N\times F}$,where the initial input $H^{(0)} = X$.

3. EXPERIMENT

3.1. Experimental Setup

To meet the data requirements of deep learning, we segmented each participant's task-state fMRI data into non-overlapping 4-second time windows. Each window was treated as an independent sample for brain network construction. Using the 90 regions defined in the Anatomical Automatic Labeling (AAL) atlas as network nodes, we computed Pearson correlation coefficients between different brain regions to construct functional connectivity networks.For binary undirected network construction, we selected a sparsity range of 5%-50% with 5% increments to comprehensively estimate topological properties across varying sparsity thresholds while minimizing spurious connections[24]. Negative correlations were excluded from analysis due to their ambiguous physiological interpretation[25].The experiment employed 10-fold cross-validation to evaluate model performance. All models were trained on an NVIDIA GeForce RTX 4090 GPU (24GB) using the PyTorch deep learning framework. The dataset was balanced between positive and negative samples and split into training and test sets at an 8:2 ratio. Model optimization used the Adam optimizer with a learning rate of 0.001 and cross-entropy loss function, trained for 100 epochs.

3.2. Result

To evaluate the impact of local features under different sparsity levels on model training, we analyzed both the local features at each specific sparsity threshold and their corresponding AUC values across the entire sparsity range. The classification model's performance was systematically assessed through 10-fold cross-validation at multiple sparsity levels, with comprehensive evaluation metrics including mean accuracy, precision, recall, and F1-score. As demonstrated in Fig. 2, the model achieved its peak classification performance at a sparsity level of 0.5, delivering outstanding results: 94% average accuracy, 95% precision, 94% recall, and 94% F1-score, indicating robust and balanced predictive capability across all performance metrics.

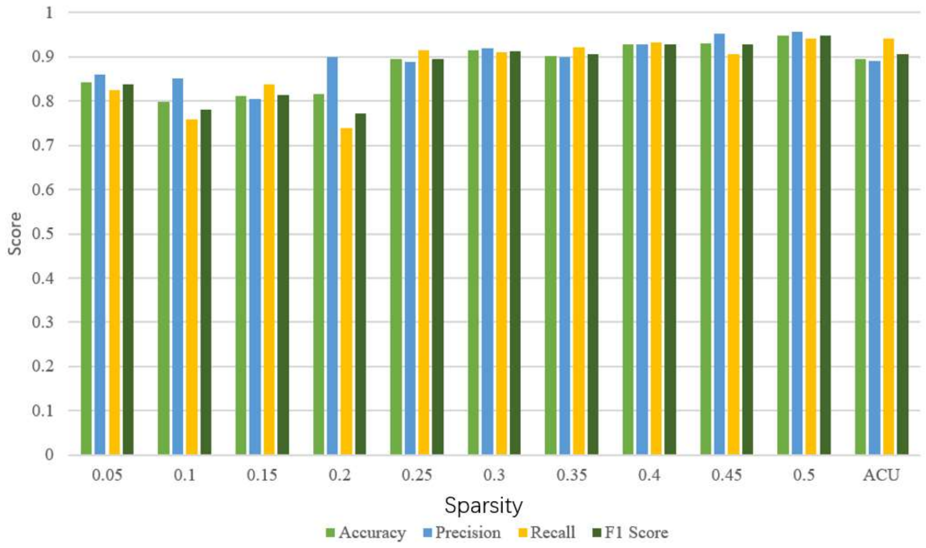

Fig. 2 Results of the Model at Different Sparsity Levels

We compared the classification performance of different feature matrices and conducted a comprehensive evaluation using mean Accuracy, Precision, Recall, and F1-Score metrics, with the results presented in Table 2. Notably, the model achieved optimal performance when combining time-domain features, frequency-domain features, and local brain network features, outperforming all other feature matrix configurations.

Table 2 Results of different feature matrices

characteristic matrix	Accuracy	Precision	Recall	F1-Score
Time Domain Features	0.8995	0.8717	0.9426	0.9057
Frequency domain features	0.7022	0.8461	0.5347	0.6553
Local features of brain network	0.9216	0.9275	0.9187	0.9231
Time Domain+ Frequency domain+ Local features of brain network	**0.9492**	**0.9579**	**0.9412**	**0.9484**

To validate the effectiveness of the GCN model, we compared it with existing baseline models for fMRI-based diagnosis of developmental dyslexia. As shown in Table 3, the GCN model achieved superior performance across all evaluation metrics, with 95% accuracy, 96% precision, 93% recall, and 95% F1-score, outperforming the other three comparative models.

Table 3 Experimental Results of Various Methods

method	Accuracy	Precision	Recall	F1-Score
SVM[26]	0.7868	0.7476	0.8587	0.7993
CNN[14]	0.8694	0.8132	0.9553	0.8786
3D-CNN[9]	0.8952	0.8955	0.8922	0.8939
GCN	**0.9522**	**0.9687**	**0.9323**	**0.9501**

3.3. Statistical Analysis

A Kolmogorov-Smirnov (K-S) test was performed to compare local brain network characteristics between the dyslexia group and control group, with results presented in Figure 3. Statistical analysis revealed significant differences ($p < 0.05$) in six local network features across multiple brain nodes, demonstrating distinct topological patterns between groups.

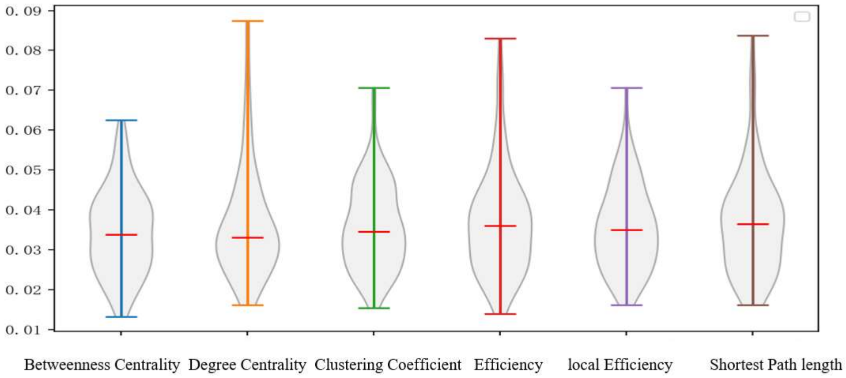

Fig. 3 K-S test results of local features in different brain regions

4. CONCLUSION

This study employed a Graph Convolutional Network (GCN) model that incorporated time-domain, frequency-domain, and local brain network features as node attributes, performing graph convolution operations to comprehensively learn spatial relationships among brain network nodes. The model achieved 94% classification accuracy in identifying individuals with developmental dyslexia (DD). With additional training data, this approach could ultimately lead to the development of neuroimaging biomarkers for dyslexia, enabling early DD diagnosis. This methodological advancement may also establish new pathways for broader clinical applications of functional magnetic resonance imaging (fMRI).

REFERENCES

[1] Peterson R L, Pennington B F J T L. Developmental dyslexia[J]. The lancet, 2012, 379(9830): 1997-2007.

[2] Li Kaiqian, Liang Dandan Brain abnormalities and early neural markers of developmental reading disorders in children at risk [J]. Advances in psychological science , 2023, 31(10): 1912.

[3] Stein J J B S. Theories about developmental dyslexia[J]. Brain sciences, 2023, 13(2): 208.

[4] Wilmot A, Hasking P, Leitão S, et al. Understanding mental health in developmental dyslexia: a scoping review[J]. International journal of environmental research and public health, 2023, 20(2): 1653.

[5] Zhang L, Xia Z, Zhao Y, et al. Recent advances in Chinese developmental dyslexia[J]. Annual Review of Linguistics, 2023, 9: 439-461.

[6] Appadurai J P, Bhargavi R J I J O C I, Intelligence N. Eye movement feature set and predictive model for dyslexia: Feature set and predictive model for dyslexia[J]. International Journal of Cognitive Informatics and Natural Intelligence (IJCINI), 2021, 15(4): 1-22.

[7] Ortiz A, Martinez-Murcia F J, Formoso M A, et al. Dyslexia detection from EEG signals using SSA component correlation and convolutional neural networks[C]//. International Conference on Hybrid Artificial Intelligence Systems, 2020: 655-664.

[8] Kohli M, Prasad T. Identifying dyslexic students by using artificial neural networks[C]//. Proceedings of the world congress on engineering, 2010: 1-4.

[9] Zahia S, Garcia-Zapirain B, Saralegui I, et al. Dyslexia detection using 3D convolutional neural networks and functional magnetic resonance imaging[J]. Computer methods and programs in biomedicine, 2020, 197: 105726.

[10] Cui Z, Xia Z, Su M, et al. Disrupted white matter connectivity underlying developmental dyslexia: a machine learning approach[J]. Human brain mapping, 2016, 37(4): 1443-1458.

[11] Płoński P, Gradkowski W, Altarelli I, et al. Multi-parameter machine learning approach to the neuroanatomical basis of developmental dyslexia[J]. Human Brain Mapping, 2017, 38(2): 900-908.

[12] Alqahtani N D, Alzahrani B, Ramzan M S J a S. Deep learning applications for dyslexia prediction[J]. Applied Sciences, 2023, 13(5): 2804.

[13] Usman O L, Muniyandi R C. CryptoDL: Predicting Dyslexia Biomarkers from Encrypted Neuroimaging Dataset Using Energy-Efficient Residue Number System and Deep Convolutional Neural Network[J]. Symmetry, 2020, 12(5): 836.

[14] Tomaz Da Silva L, Esper N B, Ruiz D D, et al. Visual explanation for identification of the brain bases for developmental dyslexia on fMRI data[J]. Frontiers in computational neuroscience, 2021, 15: 594659.

[15] Kipf T N, Welling M. Semi-supervised classification with graph convolutional networks[J]. arXiv preprint arXiv:1609.02907, 2016.

[16] Bhatti U A, Tang H, Wu G, et al. Deep learning with graph convolutional networks: An overview and latest applications in computational intelligence[J]. International Journal of Intelligent Systems, 2023, 2023(1): 8342104.

[17] Zhang L, Zhao Y, Che T, et al. Graph neural networks for image-guided disease diagnosis: A review[J]. iRADIOLOGY, 2023, 1(2): 151-166.

[18] Zhang X, Chou J, Wang F. Integrative analysis of patient health records and neuroimages via memory-based graph convolutional network[C]//. 2018 IEEE International Conference on Data Mining (ICDM), 2018: 767-776.

[19] Yin G, Chang Y, Zhao Y, et al. Automatic recognition of schizophrenia from brain-network features using graph convolutional neural network[J]. Asian Journal of Psychiatry, 2023, 87: 103687.

[20] Arya D, Olij R, Gupta D K, et al. Fusing structural and functional MRIs using graph convolutional networks for autism classification[C]//. Medical imaging with deep learning, 2020: 44-61.

[21] Yang B, Pan H, Yu J, et al. Classification of medical images with synergic graph convolutional networks[C]//. 2019 IEEE 35th International Conference on Data Engineering Workshops (ICDEW), 2019: 253-258.

[22] Jenkinson M, Beckmann C F, Behrens T E, et al. Fsl[J]. Neuroimage, 2012, 62(2): 782-790.

[23] Yin Z, Li J, Zhang Y, et al. Functional brain network analysis of schizophrenic patients with positive and negative syndrome based on mutual information of EEG time series[J]. Biomedical Signal Processing and Control, 2017, 31: 331-338.

[24] Zhu H, Qiu C, Meng Y, et al. Altered topological properties of brain networks in social anxiety disorder: a resting-state functional MRI study[J]. Scientific reports, 2017, 7(1): 43089.

[25] Murphy K, Fox M D J N. Towards a consensus regarding global signal regression for resting state functional connectivity MRI[J]. Neuroimage, 2017, 154: 169-173.

[26] Tamboer P, Vorst H, Ghebreab S, et al. Machine learning and dyslexia: Classification of individual structural neuro-imaging scans of students with and without dyslexia[J]. NeuroImage: Clinical, 2016, 11: 508-514.